Supporting Information

Efficient Harvesting and Storage of Solar Energy of an All-Vanadium Solar Redox Flow Battery with a MoS$_2$@TiO$_2$ Photoanode

Gengyu Tian,[a] Rhodri Jervis,[b] Joe Briscoe,[a] Magdalena Titirici,[c] Ana Jorge Sobrido[a],*

[a]School of Engineering and Materials Science, Materials Research Institute, Queen Mary University of London, E1 4NS, London, United Kingdom

[b]Electrochemical Innovation Lab, Department of Chemical Engineering, University College London, WC1E 7JE, United Kingdom

[c]Department of Chemical Engineering, Imperial College London, South Kensington Campus, SW7 2AZ, London, United Kingdom

Table S1. SRFB systems reported in the literature and their SCCE values.

Solar-to-chemical conversion efficiency (SCCE),	Photoanode	Cathode	Redox couples	Solar–to- output energy conversion efficiency (SOEE)
N/A	$MoS_2@TiO_2$	Carbon felt	VO^{2+}/VO_2^+ in H_2SO_4 and VO^{2+}/V^{3+} in H_2SO_4	4.78% (This work)
N/A	$BiVO_4$	Carbon on Ti foil	Br_3^-/Br in H_2SO_4 and $AQDS/AQDSH_2$ in H_2SO_4	1.25%[1]
N/A	TiO_2	Carbon paper	VO^{2+}/VO_2^+ in H_2SO_4 and V^{3+}/V^{2+} in H_2SO_4	0.6%[2]
0.021%-0.04%	$CH_3NH_3PbI_3$ (MAPbI$_3$) perovskite	Pt	ferrocenium/ferrocene (Fc$^+$/Fc) in CH_3CN and 1,4-benzoquinone semiquinone/radical anion (BQ/BQ$^-$) in CH_2Cl_2 with Tetrabutylammonium hexafluoro-phosphate (TBAPF$_6$)	N/A[3]
1.6%	pn$^+$Si/Ti/TiO$_2$/Pt	Graphite	TEMPO-4-sulfate sodium salt and $K_3Fe(CN)_6$ in NH_4Cl at pH 7	N/A[4]
0.1%	A tandem with a bare hematite photoanode and two dye-sensitized solar cells (DSSCs) connected in series	Carbon felt	I^-/I_2 in NH_4I and $AQDS/AQDSH_2$ in NH_4I	N/A[5]

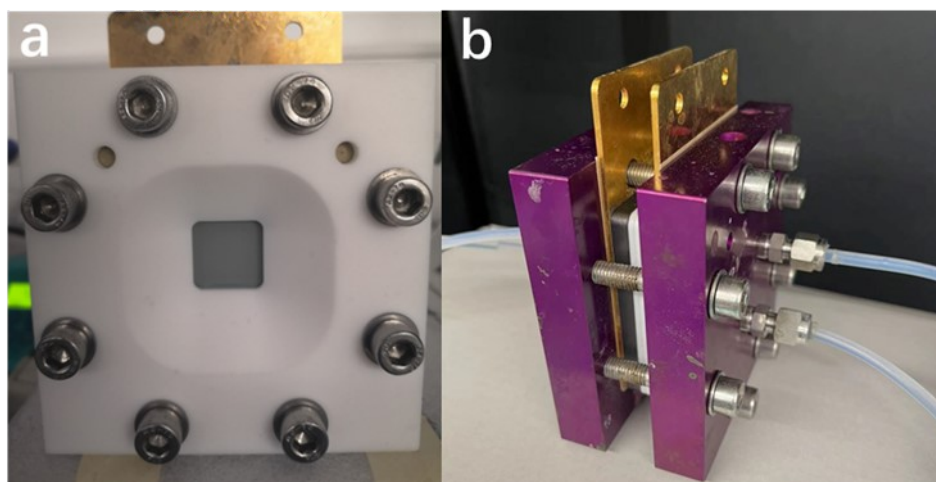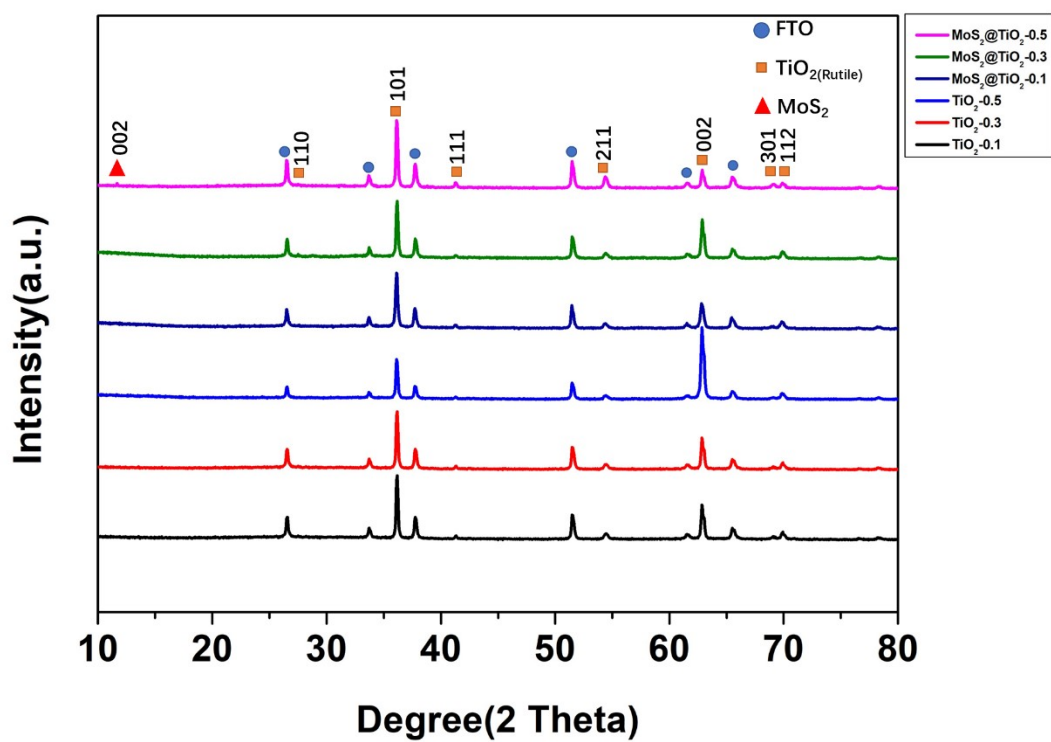| 5.9% | C/TiO$_2$/Ti/n$^+$p$^-$Si | Pt/p$^+$n$^-$Si | AQDS/AQDSH$_2$ and Br$_3^-$/Br$^-$ | 3.2%[6] |
| N/A | n-WSe$_2$ | Carbon paper | AQS/AQSH$_2$ and I$_3^-$/I$^-$ | 2.8%[7] |

Figure S1. Solar redox flow battery used for this work.

Figure S2. XRD patterns of TiO$_2$-0.1/0.3/0.5 and MoS$_2$@TiO$_2$-0.1/0.3/0.5.
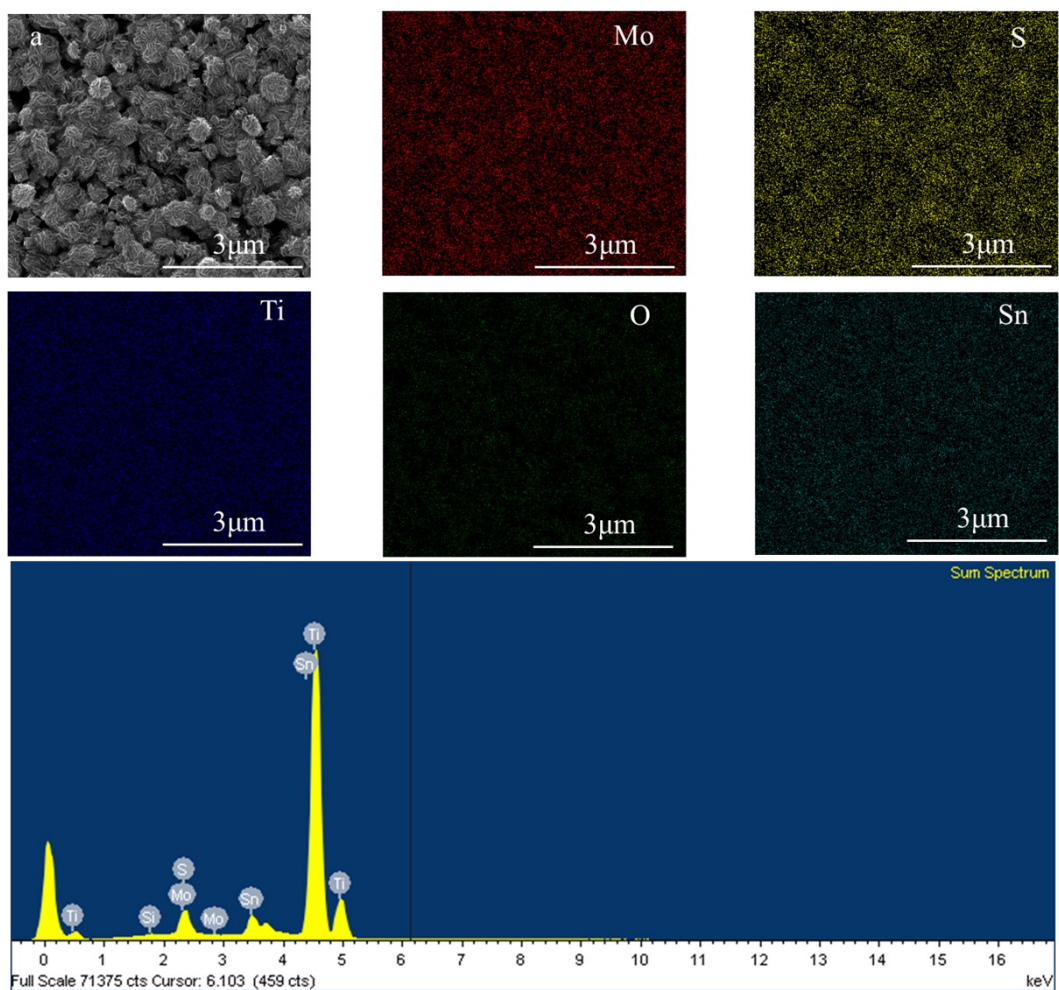
Figure S3. EDS images and spectrum of MoS$_2$@TiO$_2$-0.5.
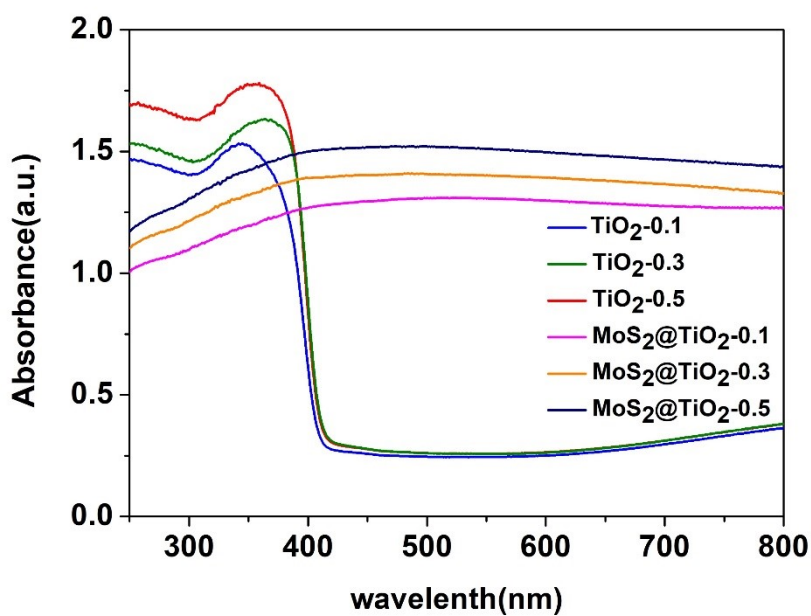

Figure S4. UV-vis spectra of TiO$_2$-0.5 and MoS$_2$@TiO$_2$-0.5 using back-illumination

mode.
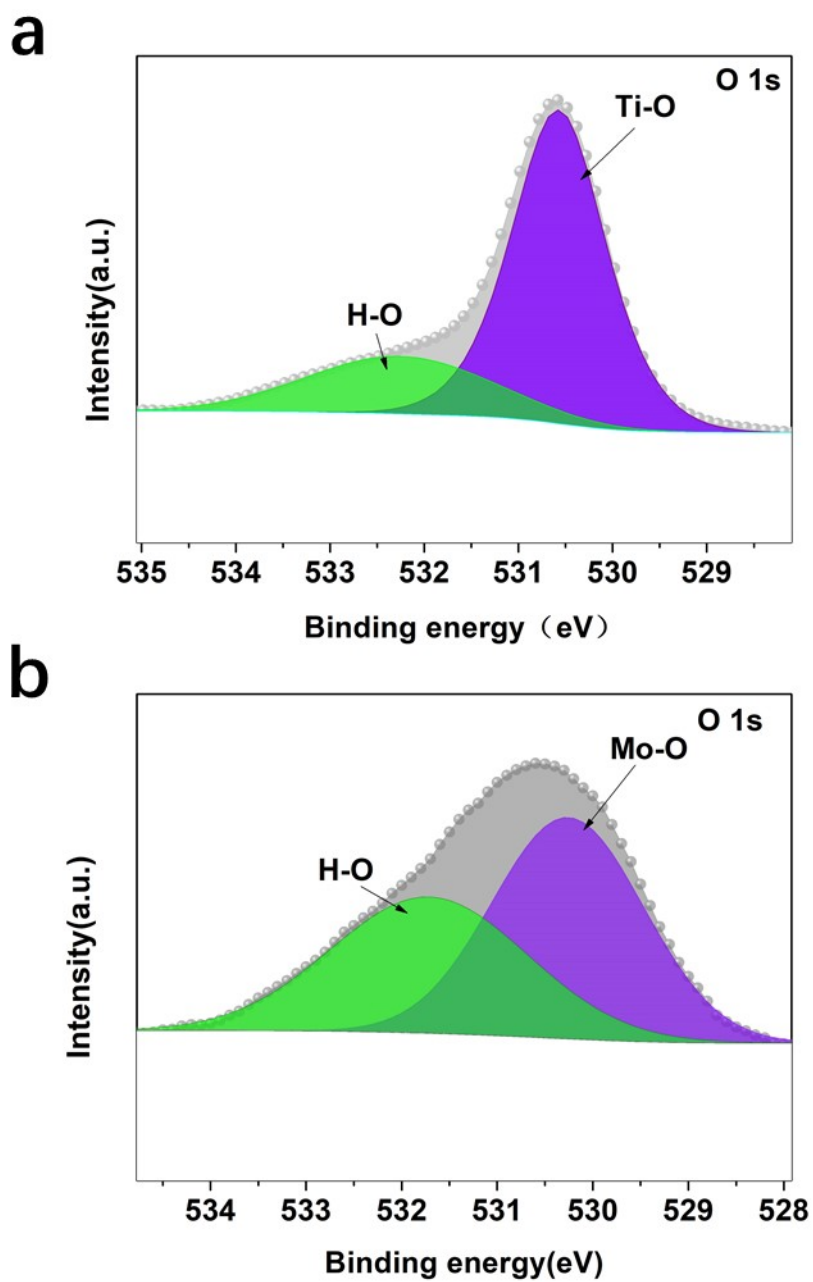
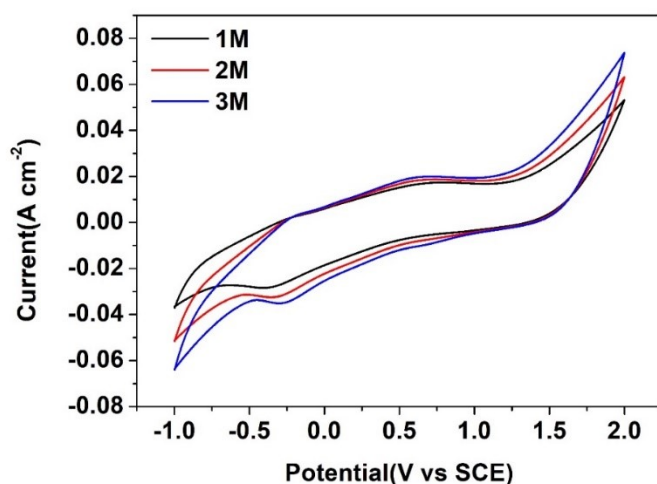Figure S5. XPS spectra of O 1s from (a) TiO_2-0.5, and (b) $MoS_2@TiO_2$-0.5.

Figure S6. CV (scan rate 100 mV s^{-1}) of 1.0 M/2.0 M/3.0 M sulfuric acid in three electrode system. In this setup, carbon felt was employed as working electrode, and KCl saturated calomel Hg$_2$Cl$_2$ electrode (SCE) and Pt coil were used as reference and counter electrodes, respectively.
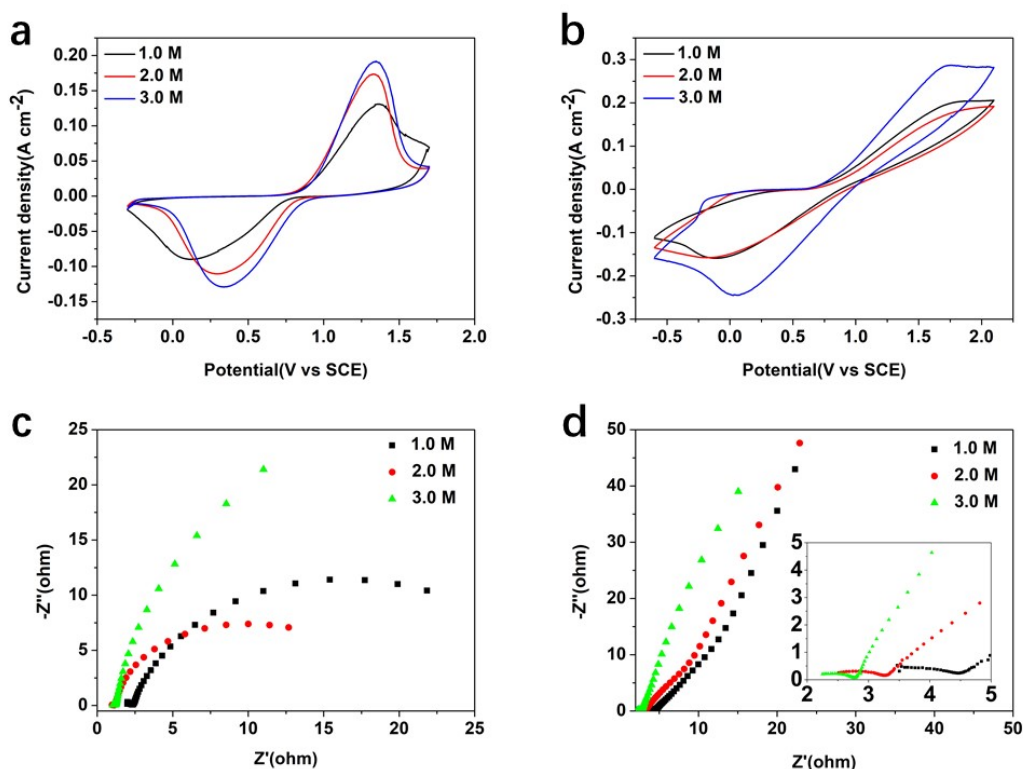

Figure S7. CV (scan rate 10mV s^{-1}) of (a) 0.1 M V^{4+} and (b) 1.0 M V^{4+} with 1.0 M/2.0 M/3.0 M sulfuric acid and EIS (AC 10mV) of (c) 0.1 M V^{4+} and (d) 1.0 M V^{4+} with 1.0 M/2.0 M/3.0 M sulfuric acid in three electrode system. In this setup, carbon fiber is the working electrode, a KCl saturated calomel Hg$_2$Cl$_2$ electrode (SCE) and a Pt coil were used as reference and counter electrodes, respectively.

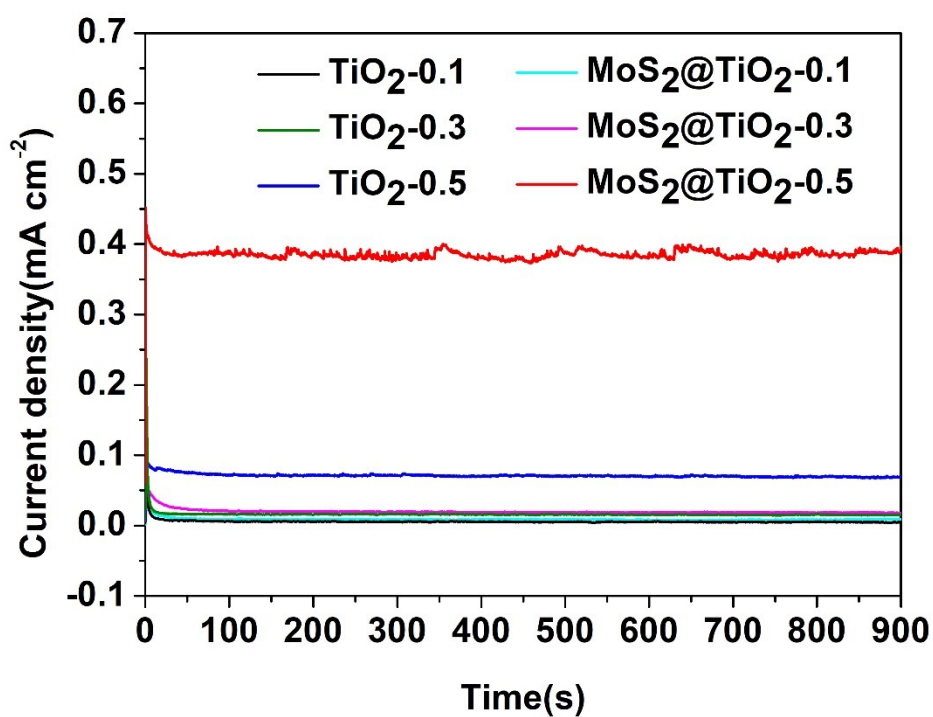Figure S8. Photocurrent density in a solar redox flow cell configuration of photoanodes TiO_2-0.1, TiO_2-0.5 and $MoS_2@TiO_2$-0.5 (100 mW cm^{-2} (AG1.5) in 0.1 M V^{4+} with 3.0 M H_2SO_4 2.5 mL min^{-1} flow rate) using thermal treated carbon felt as cathode.
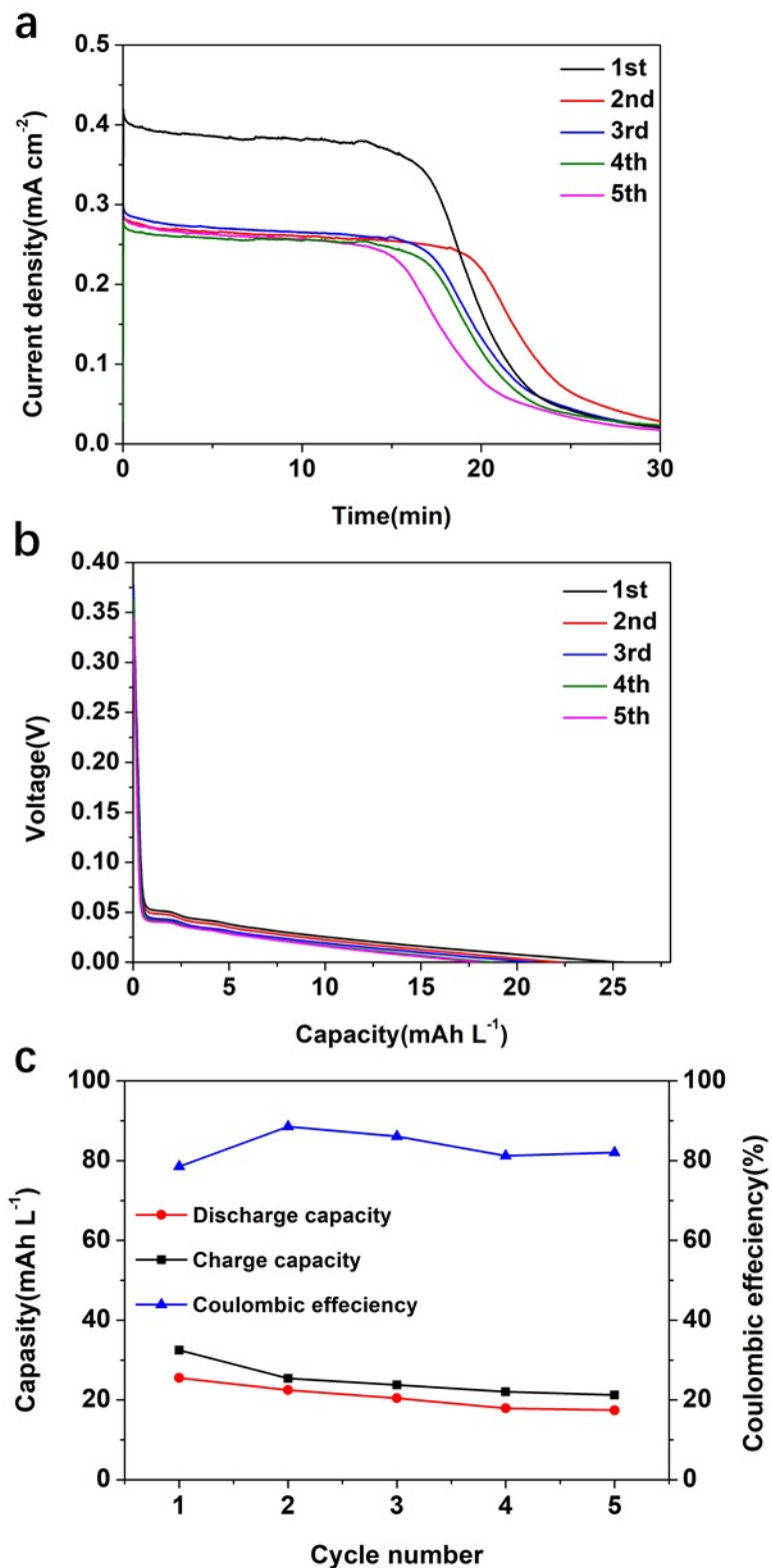
Figure S9. (a) Cyclic photocharge, (b) discharge of $MoS_2@TiO_2$-0.5 and (c) the capacity and coulombic efficiency in the vanadium ion concentration of 0.1 M V^{4+}. The discharge current density is 0.4 mA cm^{-2}. (100 mW cm^{-2}(AG1.5) with 3.0 M H_2SO_4 and 2.5 mL min^{-1} flow rate).
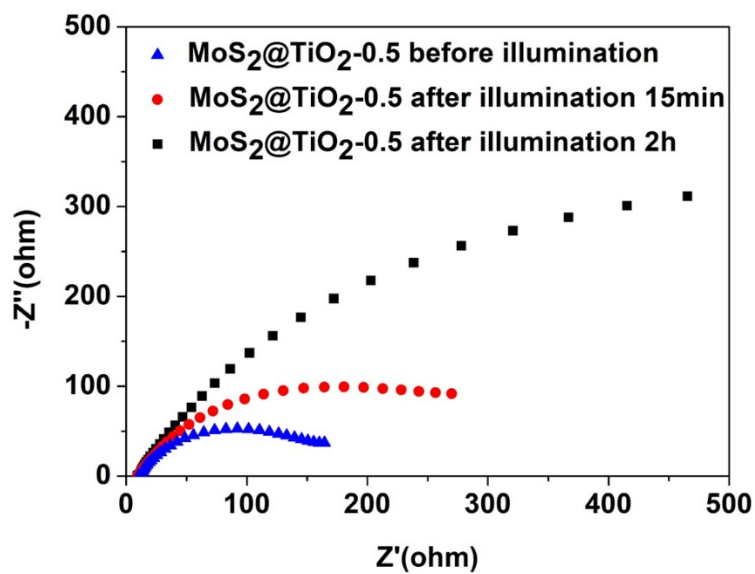
Figure S10. EIS of SRFB in two electrode system under dark condition (1.0 M with V^{3+}/V^{4+} catholyte, V^{4+}/V^{5+} anolyte, carbon felt cathode and Nafion membrane).
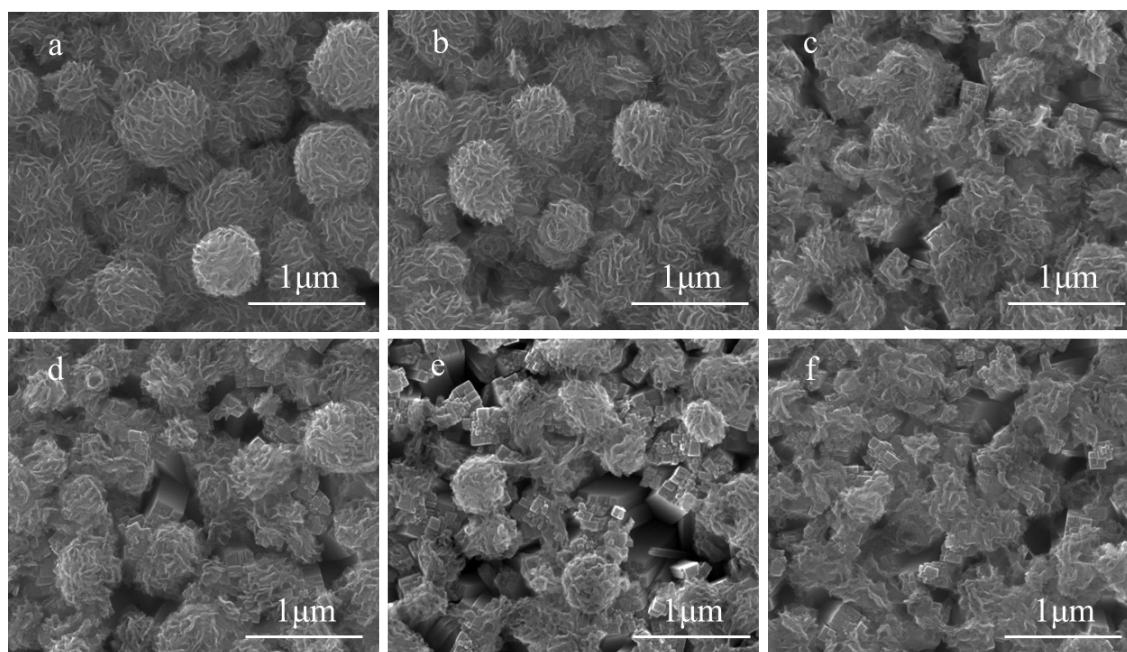

Figure S11. SEM of MoS$_2$@TiO$_2$-0.5 in 0.1M V^{4+} (a) before photocharge, (b) after 1st full photocharge cycle and (c)after 2nd full photocharge cycle (d) after 3rd full photocharge cycle (e) after 4th full photocharge cycle, (f) after 5th full photocharge cycle.
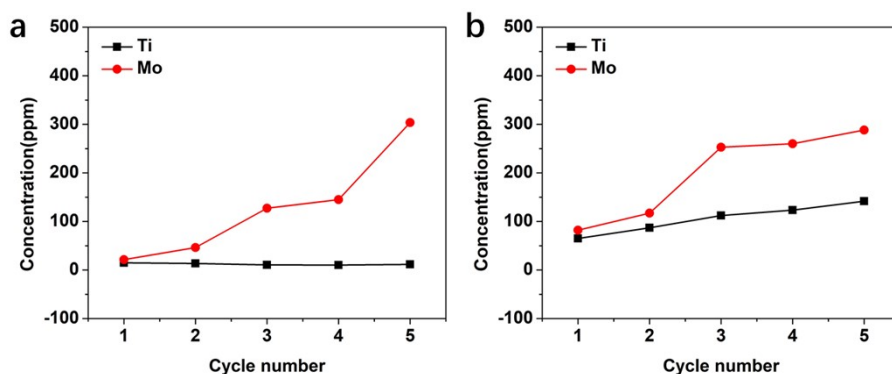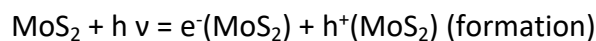
Figure S12. Ti and Mo element concentration (ICP-MS) in the positive-side electrolyte of (a) 0.1 M and (b) 1.0 M V^{4+} with time of cycling.
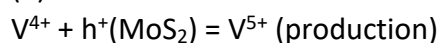
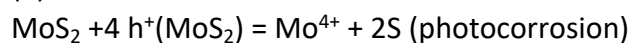Equation S1. When illuminated, the photoexcitation and electron transfer of MoS_2 can be represented as follows:

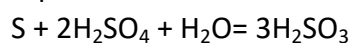$MoS_2 + h\nu = e^-(MoS_2) + h^+(MoS_2)$ (formation)

(1)

$e^-(MoS_2) + h^+(MoS_2) = MoS_2 + h\nu$ (recombination)

(2)

$V^{4+} + h^+(MoS_2) = V^{5+}$ (production)
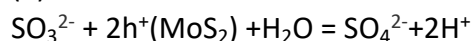
(3)

$MoS_2 + 4 h^+(MoS_2) = Mo^{4+} + 2S$ (photocorrosion)

(4)
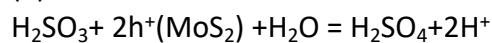
Where $e^-(MoS_2)$ and $h^+(MoS_2)$ means e^- and h^+ in MoS_2 which including e^- and h^+ from both MoS_2 and TiO_2. The remaining reaction in high concentration of H_2SO_4 can be represented as follows:

$S + 2H_2SO_4 + H_2O = 3H_2SO_3$

(5)

$SO_3^{2-} + 2h^+(MoS_2) + H_2O = SO_4^{2-} + 2H^+$
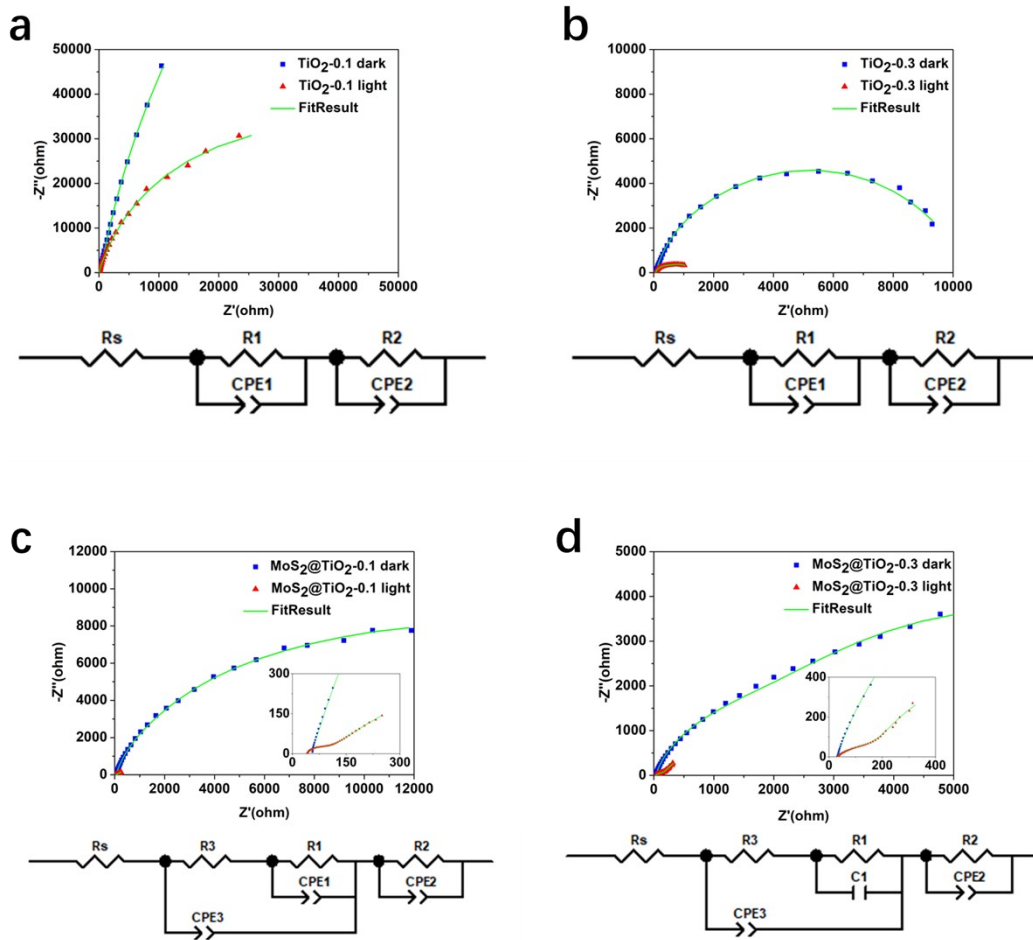
(6)

$H_2SO_3 + 2h^+(MoS_2) + H_2O = H_2SO_4 + 2H^+$

(7)

Figure S13. EIS in 0.1 M V^{4+} of (a) TiO_2-0.1 (b) TiO_2-0.3 (c) $MoS_2@TiO_2$-0.1 and (d) $MoS_2@TiO_2$-0.3.

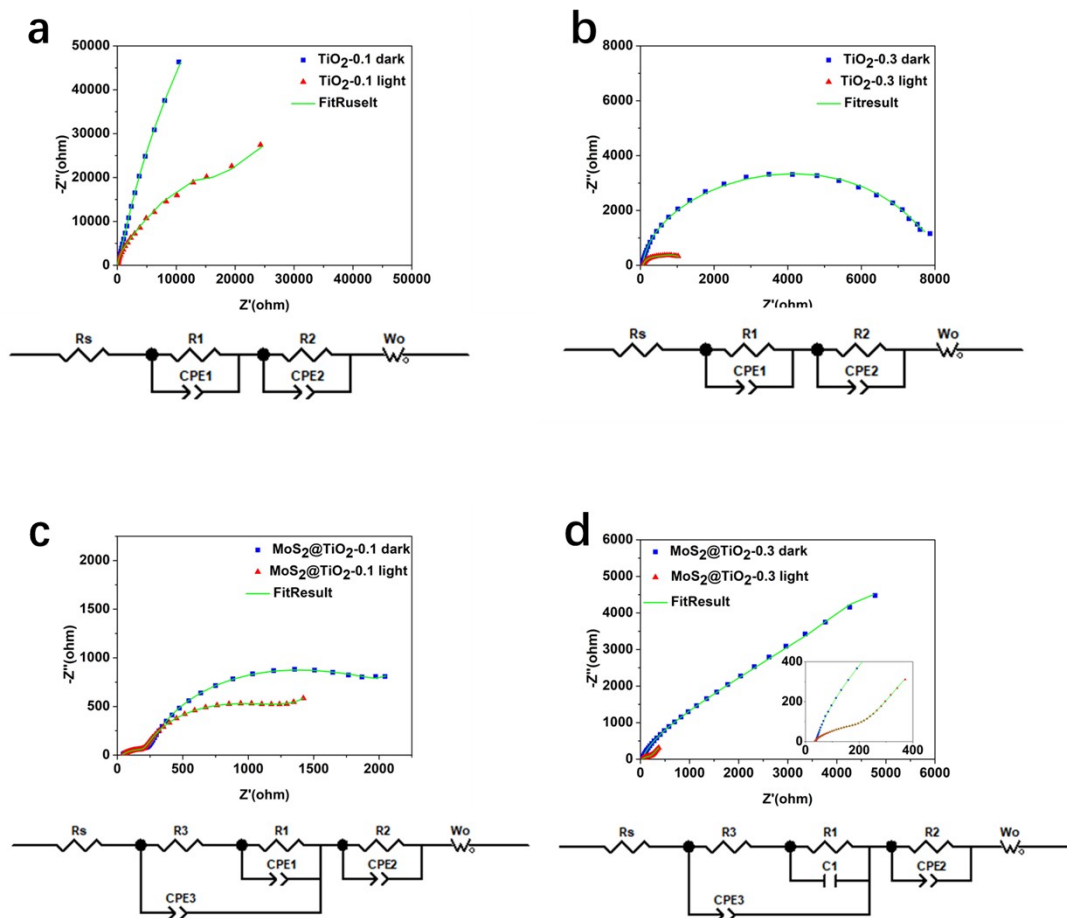Figure S14. EIS in 1.0 M V^{4+} of (a) TiO_2-0.1 (b) TiO_2-0.3 (c) $MoS_2@TiO_2$-0.1 and (d) $MoS_2@TiO_2$-0.3.

Reference

1.   Zhou, Y.,Zhang, S.,Ding, Y.,Zhang, L.,Zhang, C.,Zhang, X.,Zhao, Y.and Yu, G. *Advanced Materials,* 2018, **30**, 1802294.

2.   Wei, Z.,Shen, Y.,Liu, D.and Liu, F. *Scientific reports,* 2017, **7**, 1-9.

3.   Lin, G.,Almakrami, H.,Emran, H.,Ruthen, A.,Hu, J.,Wei, Z.and Liu, F. *ChemPhysChem,* 2021, **22**, 1193-1200.

4.   Wedege, K.,Bae, D.,Dražević, E.,Mendes, A.,Vesborg, P. C.and Bentien, A. *RSC advances,* 2018, **8**, 6331-6340.

5.   Khataee, A.,Azevedo, J.,Dias, P.,Ivanou, D.,Dražević, E.,Bentien, A.and Mendes, A. *Nano Energy,* 2019, **62**, 832-843.

6.   Liao, S.,Zong, X.,Seger, B.,Pedersen, T.,Yao, T.,Ding, C.,Shi, J.,Chen, J.and Li, C. *Nature communications,* 2016, **7**, 1-8.

7.   McKone, J. R.,DiSalvo, F. J.and Abruña, H. D. *Journal of Materials Chemistry A,* 2017, **5**, 5362-5372.